Joint Time-Delay and Frequency Estimation using Parallel Factor Analysis

Yuntao Wu*, H. C. So† and Yunsong Tan*

* School of Computer Science and Engineering, Wuhan Institute of Technology, Wuhan, 430073, China

† Department of Electronic Engineering, City University of Hong Kong Kowloon, Hong Kong

January 12, 2009

Abstract : In this paper, the problem of joint time-delay and frequency estimation of multiple sinusoidal signals received at two separated sensors is addressed. By formulating the estimation problem with the use of the parallel factor analysis framework, the corresponding state transition and observation matrices are updated in an iterative manner according to alternating least squares, from which the time-delay and frequencies are then estimated. Computer simulations are included to demonstrate the effectiveness of the proposed algorithm.

Indexing terms : frequency estimation, time-delay estimation, fast algorithm, parallel factor analysis

1 Introduction

Time-delay estimation between noisy versions of a source signal received at spatially separated sensors has been an active research topic in the literature [1]. In this paper, we consider that the source signal is a sinusoidal signal and the objective is to find the time-delay and frequency parameters from the received sensor outputs [2]-[3]. The joint time-delay and frequency estimation problem has applications such as analysis of thalamocortical seizure pathways [4], frequency-shift keying demodulation using multiple data segments [5] and speaker localization [6]. Without loss of generality, we consider two sensor outputs which are modeled as:

$$
\begin{aligned}
r_1(n) &= s(n) + q_1(n) \\
r_2(n) &= s(n-D) + q_2(n), \quad n = 0, 1, \cdots, N-1
\end{aligned}
\tag{1}
$$

where $s(n) = \sum_{m=1}^{P} \alpha_m \exp(j\omega_m n)$ consists of P complex sinusoids. The P is assumed known, the complex amplitudes and frequencies are denoted by $\{\alpha_m\}$ and $\{\omega_m\}$, respectively, which are unknown deterministic constants, with $\omega_i \neq \omega_j$ for $i \neq j$. The additive noises $q_1(n)$ and $q_2(n)$ are uncorrelated zero-mean complex white Gaussian processes with unknown variances σ_q^2. The parameter D represents the difference in arrival times at the two receivers and N is the number of samples collected at each channel. Given $r_1(n)$ and $r_2(n)$, the task is to estimate D and $\{\omega_m\}$.

A subspace-based method [2] has been developed for joint delay and frequency estimation and the estimates are obtained using the eigenvalues and eigenvectors of a matrix derived from the covariance matrices of the received signals. By utilizing the state-space parameterization, an improved joint estimator which provides higher accuracy at the expense of larger computational complexity is devised in [3]. Parallel factor (PARAFAC) analysis [7], which is rooted in psychometrics and chemometrics, is a useful tool for low-rank decomposition of three- and higher way arrays. In this paper, we show that the state-space realization [3] of (1) can be modeled as a third-order tensor, which fits into the PARAFAC model. With the use of alternating least squares (ALS) on the trilinear PARAFAC model, we estimate the corresponding state transition and observation matrices from which the time-delay and frequencies are then obtained. It is demonstrated that the PARAFAC method is superior to [3] in terms of threshold performance and computational complexity.

2 Proposed Method

Given the two sensor outputs, we construct $\mathbf{x}(n)$ which has the form of

$$\mathbf{x}(n) = [r_1(n), r_1(n+1), \cdots, r_1(n+M-1), r_2(n), r_2(n+1), \cdots, r_2(n+M-1)]^T, \quad n = 0, 1, \cdots, K-1 \tag{2}$$

where $K = N - M + 1$ and $2M$ is the vector length, and both M and K are larger than P. Following [3], the state-space model of (2) is

$$\begin{aligned} \mathbf{S}(n+1) &= \mathbf{\Phi}\mathbf{S}(n) \\ \mathbf{x}(n) &= \mathbf{B}\mathbf{S}(n) + \mathbf{Q}(n) \end{aligned} \tag{3}$$

where

$$\mathbf{S}(n) = \left[\alpha_1 e^{j\omega_1 n}, \alpha_2 e^{j\omega_2 n}, \cdots, \alpha_P e^{j\omega_P n}\right]^T$$

$$\mathbf{\Phi} = \mathrm{diag}(e^{j\omega_1}, e^{j\omega_2}, \cdots, e^{j\omega_P})$$

$$\mathbf{B} = \left[\mathbf{A}^T \quad (\mathbf{A}\mathbf{\Delta})^T\right]^T$$

$$\mathbf{A} = \begin{bmatrix} 1 & 1 & \cdots & 1 \\ e^{j\omega_1} & e^{j\omega_2} & \cdots & e^{j\omega_P} \\ \vdots & \vdots & \vdots & \vdots \\ e^{j\omega_1(M-1)} & e^{j\omega_2(M-1)} & \cdots & e^{j\omega_P(M-1)} \end{bmatrix}$$

$$\mathbf{\Delta} = \mathrm{diag}(e^{-jD\omega_1}, e^{-jD\omega_2}, \cdots, e^{-jD\omega_P})$$

$$\mathbf{Q}(n) = [q_1(n), q_1(n+1), \cdots, q_1(n+M-1), q_2(n), q_2(n+1), \cdots, q_2(n+M-1)]^T$$

Denoting $\mathbf{X}_l(n) = \mathbf{x}(n+l), n = 1, \cdots, K-L+1$, we can express (3) as:

$$\mathbf{X}_l(n) = \mathbf{B}\mathbf{\Phi}_l\mathbf{S}(n) + \mathbf{Q}(n+l), \quad l = 0, 1, \cdots, L-1 \tag{4}$$

where $\mathbf{\Phi}_l = \mathbf{\Phi}^l = \mathrm{diag}(e^{jl\omega_1}, \cdots, e^{jl\omega_P})$. To utilize the PARAFAC analysis, we let $\mathbf{H}$ be the $L \times P$ matrix whose $(l+1)$-th row is the diagonal element of $\mathbf{\Phi}_l$, and denote $\mathbf{D}_l(\mathbf{H})$ as the diagonal matrix containing the $(l+1)$-th row of $\mathbf{H}$, that is, $\mathbf{D}_l(\mathbf{H}) = \mathbf{\Phi}_l$, to rewrite (4) as

$$\mathbf{X}_l(n) = \mathbf{B}\mathbf{D}_l(\mathbf{H})\mathbf{S}(n) + \mathbf{Q}(l+n), \quad l = 0, \cdots, L-1. \tag{5}$$

Assuming that $L > P$ so that $\mathbf{H}$ is a tall matrix. Temporarily ignoring the noise term, and letting $x_{l,k,i}$ be the (k,i) entry of $\mathbf{X}_l(n)$, we have:

$$x_{l,k,i} = \sum_{m=1}^{P} b_{k,m} h_{l,m} s_{m,i} \tag{6}$$

where $b_{k,m}$, $h_{l,m}$ and $s_{m,i}$ represent the (k,m) entry of $\mathbf{B}$, (l,m) entry of $\mathbf{H}$ and (m,i) entry of $\mathbf{S}(n)$, respectively. The form of (6) is commonly known as the PARAFAC model [7]. The perfect symmetry of the trilinearity of (6) allows two revealing data rearrangements, which can be interpreted as "slicing" the $L \times 2M \times (K-L+1)$ three-way array $\mathbf{X}(l,k,i) \triangleq \mathbf{X}_l(k,i)$ along different dimensions. In particular, we have

$$\mathbf{Y}_k \triangleq \mathbf{X}(:,k,:) \quad = \quad \mathbf{S}(n)^T\mathbf{D}_l(\mathbf{B})\mathbf{H}^T, \quad k = 1, 2, \cdots, 2M \tag{7}$$

and

$$\mathbf{Z}_i \triangleq \mathbf{X}(:,:,i) \quad = \quad \mathbf{H}\mathbf{D}_i(\mathbf{S}(n)^T)\mathbf{A}^T \quad i = 1, \cdots, K-L+1 \tag{8}$$

We employ the ALS technique to fit the trilinear models of (5), (7) and (8), because of its advantages of guaranteed convergence, relative simplicity and accurate estimation performance when the data are not ill-conditioned [7]. From the first way of slicing the data, the least squares (LS) fit corresponds to minimizing:

$$\left\| \begin{bmatrix} \mathbf{X}_0(n) \\ \vdots \\ \mathbf{X}_{L-1}(n) \end{bmatrix} - \begin{bmatrix} \mathbf{B}\mathbf{D}_0(\mathbf{H}) \\ \vdots \\ \mathbf{B}\mathbf{D}_{L-1}(\mathbf{H}) \end{bmatrix} \mathbf{S}(n) \right\|^2 \tag{9}$$

It follows that the conditional LS estimate of $\mathbf{S}(n)$, denoted by $\hat{\mathbf{S}}(n)$, is:

$$\hat{\mathbf{S}}(n) = \begin{bmatrix} \hat{\mathbf{B}}\mathbf{D}_0(\hat{\mathbf{H}}) \\ \vdots \\ \hat{\mathbf{B}}\mathbf{D}_{L-1}(\hat{\mathbf{H}}) \end{bmatrix}^{\#} \begin{bmatrix} \mathbf{X}_0(n) \\ \vdots \\ \mathbf{X}_{L-1}(n) \end{bmatrix} \tag{10}$$

where $(.)^{\#}$ stands for pseudo-inverse while $\hat{\mathbf{B}}$ and $\hat{\mathbf{H}}$ represent the previously obtained estimates of $\mathbf{B}$ and $\mathbf{H}$, respectively. Similarly, from the second way of slicing the three-dimensional data, the conditional LS estimate of $\mathbf{H}$ is determined from:

$$\hat{\mathbf{H}}^T = \begin{bmatrix} \hat{\mathbf{S}}(n)^T\mathbf{D}_0(\hat{\mathbf{B}}) \\ \vdots \\ \hat{\mathbf{S}}(n)^T\mathbf{D}_{L-1}(\hat{\mathbf{B}}) \end{bmatrix}^{\#} \begin{bmatrix} \mathbf{Y}_1 \\ \vdots \\ \mathbf{Y}_{2M} \end{bmatrix} \tag{11}$$

Finally, from the third way of slicing the data, it follows that the conditional LS update for $\mathbf{B}$ is:

$$\hat{\mathbf{B}}^T = \begin{bmatrix} \hat{\mathbf{H}}\mathbf{D}_1(\hat{\mathbf{S}}(n)^T) \\ \vdots \\ \hat{\mathbf{H}}\mathbf{D}_{K-L+1}(\hat{\mathbf{S}}(n)^T) \end{bmatrix}^{\#} \begin{bmatrix} \mathbf{Z}_1 \\ \vdots \\ \mathbf{Z}_{K-L+1} \end{bmatrix} \tag{12}$$

The initial estimates in the iterative procedure of (10)−(12) can be provided by the single-invariance ESPRIT [8] algorithm. Note that global monotone convergence to at least a local minimum is guaranteed in the trilinear ALS regression [7]. Moreover, the matrices $\mathbf{S}(n)$, $\mathbf{H}$ and $\mathbf{B}$ are of full rank of P when $\omega_i \neq \omega_j$ for $i \neq j$, and hence the identifiability condition is satisfied [7].

Using the structure of $\hat{\mathbf{H}}$, the estimate of $\mathbf{\Phi}$, denoted by $\hat{\mathbf{\Phi}}$, is obtained as:

$$\hat{\mathbf{\Phi}} = \hat{\mathbf{H}}^{\#}(1:L-1,:)\hat{\mathbf{H}}(2:L,:) \tag{13}$$

Then the frequency estimates, denoted by $\{\hat{\omega}_m\}$, are given by the phases of the diagonal elements of $\hat{\mathbf{\Phi}}$:

$$\hat{\omega}_m = \angle\hat{\mathbf{\Phi}}(m,m), \qquad m = 1, 2, \cdots, P \tag{14}$$

On the other hand, the estimate of $\mathbf{\Delta}$, $\hat{\mathbf{\Delta}}$, is calculated as

$$\hat{\mathbf{\Delta}} = \hat{\mathbf{B}}^{\#}(1:M,:)\hat{\mathbf{B}}(M+1:2M,:) \tag{15}$$

Finally, the delay estimate, denoted by $\hat{D}$, is determined using the estimated frequencies and the diagonal elements of $\hat{\boldsymbol{\Delta}}$ in a weighted average manner:

$$\hat{D} = \frac{\sum_{m=1}^{P} \angle \hat{\boldsymbol{\Delta}}(m,m)}{-\sum_{m=1}^{P} \hat{\omega}_m} \tag{16}$$

Regarding the main computational requirement, the complexity of the proposed algorithm is of $o(3\mathcal{I}(P^3 + 2PLM(N - M - L + 2)))$ [7] where $\mathcal{I}$ denotes the number of iterations in (10)$-$(12). While the computational complexity of the subspace-based method [3] is of $o((2ML)^2(N-M+1)+8M^3L^3)$. When the value of $\mathcal{I}$ is small, the proposed method will be much more computationally attractive than that of [3].

3 Simulation Results

Computer simulations have been conducted to evaluate the joint time-delay and frequency estimation performance of the proposed scheme in the presence of white Gaussian noise by comparing with the subspace-based method [3] and Cramér-Rao lower bound (CRLB). The number of iterations in the PARAFAC algorithm is $\mathcal{I} = 5$ and the initial parameter estimates are provided by the ESPRIT algorithm [8]. Note that larger values for $\mathcal{I}$ have been tried but no significant improvement is observed. The source signal is of the form $s(n) = \alpha_1 e^{j\omega_1 n} + \alpha_2 e^{j\omega_2 n}$ with $\alpha_1 = \alpha_2 = 1/\sqrt{2}$, $\omega_1 = 0.2\pi$ rad/s and $\omega_2 = 0.4\pi$ rad/s. The sampling interval is 1s and the time-delay D is selected to be 1.7s. Different signal-to-noise ratio (SNR) conditions are obtained by proper scaling of the noise sequences. The number of samples is $N = 100$, and $M = 25$ and $L = 4$ are assigned. All results provided are averages of 500 independent runs. Figures 1 to 3 plot the mean square error performance of the frequency and time-delay estimates versus SNR. At lower SNRs, the proposed method is superior to the subspace scheme particularly for the frequency estimates. It is because the latter approach is based on the splitting the measurement space into signal subspace and noise subspace and generally gives a higher threshold SNR value. For higher SNRs, the proposed and subspace algorithms have similar estimation performance which is close to the corresponding CRLBs. Since the proposed method has a smaller threshold SNR, it has a larger SNR operation range. The major complexities of the PARAFAC and subspace methods are $o(438, 120)$ and $o(11, 040, 000)$, respectively, indicating that the former is much more computationally efficient.

4 Conclusion

A novel joint estimation algorithm for time-delay and frequencies of multiple sinusoidal signals received at two sensors has been developed. Our approach combines the state-space model and parallel factor (PARAFAC) analysis to form three-way arrays with the use of the array outputs. The frequency estimates are obtained directly from the state transition matrix while the delay is determined using the observation matrix and the estimated frequencies. It is shown that the proposed PARAFAC is superior to the subspace-based method [3] in terms of threshold performance and computational requirement.

Acknowledgement

The work described in this paper was jointly supported by a grant from the National Nature Science Foundation of China (Project No. 60802046) and a grant from CityU (Project No. 7002132).

References

[1] G.C.Carter, *Coherence and Time Delay Estimation: An Applied Tutorial for Research, Development, Test and Evaluation Engineers*, IEEE press, 1993

[2] G.Liao, H.C.So and P.C.Ching, "Joint time delay and frequency estimation of multiple sinusoids," *Proc. IEEE Int. Conf. Acoust. Speech, Signal Processing*, vol.5, pp.3121-3124, May 2001, Salt Lake City, Utah, USA

[3] Y.Wu, H.C.So and P.C.Ching, "Joint time-delay and frequency estimation via state-space realization," *IEEE Signal Processing Letters*, vol.10, no.11, pp.339-342, Nov. 2003

[4] D.L.Sherman, Y.C.Tsai, L.A.Rossell, M.A.Mirski and N.V.Thakor, "Narrowband delay estimation for thalamocortical epileptic seizure pathways," *Proc. IEEE Int. Conf. Acoust. Speech, Signal Processing*, vol.5, pp.2939-2942, May 1995, Detroit, Michigan, USA

[5] J.A.Sills and Q.R.Black, "Frequency estimation from short pulses of sinusoidal signals," *Proc. IEEE MILCOM '96*, vol.3, pp.979-983, 1996, McLean, VA, USA

[6] L.Y.Ngan, Y.Wu, H.C.So, P.C.Ching and S.W.Lee, "Joint time delay and pitch estmation for speaker localization," *Proceedings of the IEEE International Symposium on Circuits and Systems*, vol.3, pp.722-725, May 2003, Bangkok, Thailand

[7] R.Bro, "PARAFAC: Tutorial and applications," *Chemometrics Intell. Lab. Syst.*, vol.38, pp.149-171, 1997

[8] R.Roy and T.Kailath, "ESPRIT - Estimation of signal parameter via rotational invariance techniques," *IEEE Trans. Acoust. Speech, Signal Processing*, vol.37, no.7, pp.984-995, July 1989

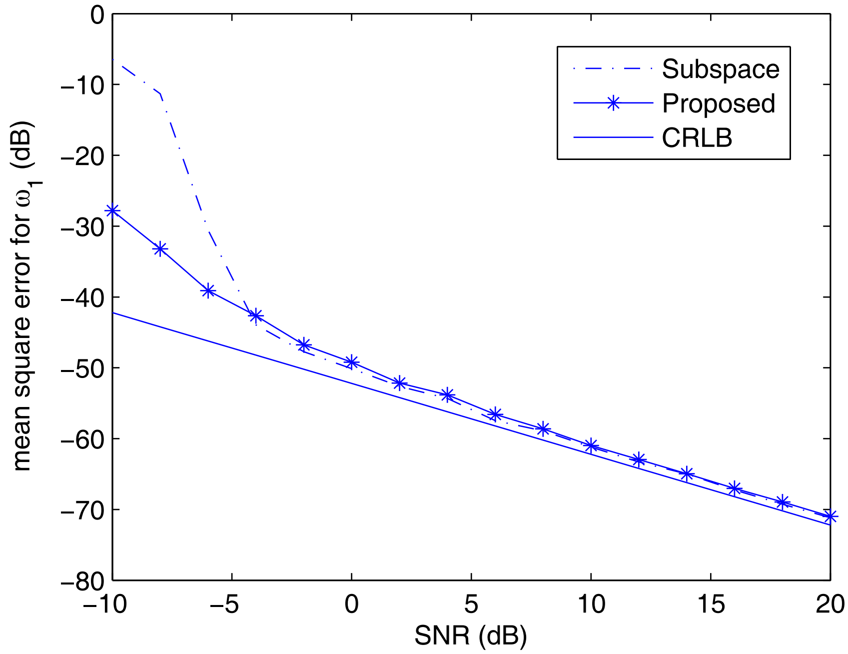

Fig.1 Mean square error for ω_1 versus SNR

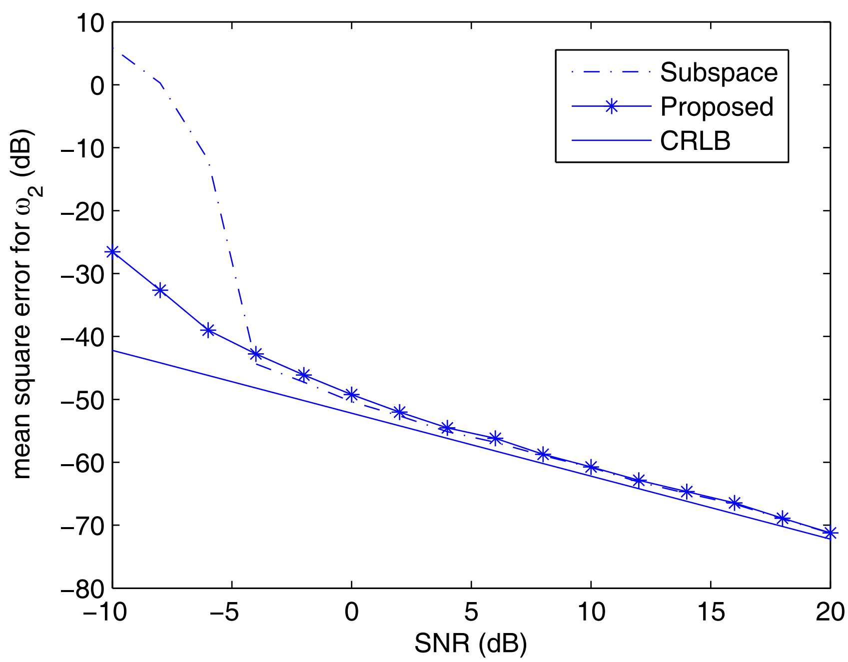

Fig.1 Mean square error for ω_2 versus SNR

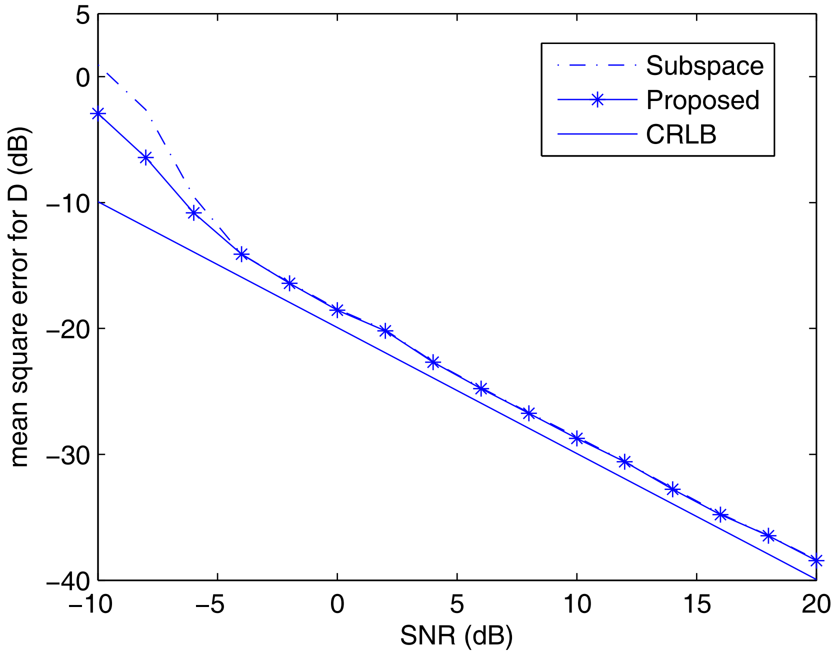

Fig.1 Mean square error for D versus SNR